Osteoarthritis and Cartilage 23 (2015) 1412–1420

Osteoarthritis and Cartilage

OARSI OSTEOARTHRITIS RESEARCH SOCIETY INTERNATIONAL

Depletion of SIRT6 causes cellular senescence, DNA damage, and telomere dysfunction in human chondrocytes

K. Nagai, T. Matsushita*, T. Matsuzaki, K. Takayama, T. Matsumoto, R. Kuroda, M. Kurosaka

Department of Orthopaedic Surgery, Kobe University Graduate School of Medicine, 7-5-1, Kusunoki-cho, Chuo-ku, Kobe, 650-0017, Japan

ARTICLE INFO

Article history:
Received 20 June 2014
Accepted 18 March 2015

Keywords:
Sirtuin
SIRT6
Chondrocyte
Senescence
DNA damage
Telomere dysfunction

SUMMARY

Objective: SIRT6, a member of the sirtuin family of nicotinamide adenine dinucleotide (NAD^+)-dependent protein deacetylases, has been implicated as a key factor in aging-related diseases. However, the role of SIRT6 in chondrocytes has not been fully explored. The purpose of this study was to examine the role of SIRT6 in human chondrocytes by inhibiting SIRT6 *in vitro*.

Design: First, the localization of SIRT6 and proliferation cell nuclear antigen (PCNA) in human cartilages was examined by immunohistochemistry. Next, SIRT6 was depleted by RNA interference (RNAi), and the effect of SIRT6 depletion on changes in gene expression, protein levels, proliferation, and senescence in human chondrocytes was assessed. Furthermore, to detect DNA damage and telomere dysfunction, γH2AX foci and telomere dysfunction-induced foci (TIFs) were examined using immunofluorescence microscopy. The protein levels of two mediators for DNA damage induced-senescence, p16 and p21, were examined by western blotting.

Results: Immunohistochemical analysis showed SIRT6 was preferentially expressed in the superficial zone chondrocytes and PCNA-positive cluster-forming chondrocytes in the osteoarthritic cartilage tissue samples. Real-time PCR analysis showed that matrix metalloproteinase 1 (*MMP-1*) and *MMP-13* mRNA were significantly increased by SIRT6 inhibition. Moreover, SIRT6 inhibition significantly reduced proliferation and increased senescence associated β-galactosidase (SA-β-Gal)-positive chondrocytes; it also led to increased p16 levels. Immunofluorescence microscopy showed that γH2AX foci and TIFs were increased by SIRT6 inhibition.

Conclusion: Depletion of SIRT6 in human chondrocytes caused increased DNA damage and telomere dysfunction, and subsequent premature senescence. These findings suggest that SIRT6 plays an important role in the regulation of senescence of human chondrocytes.

Introduction

Osteoarthritis (OA), a joint disease that often affects aged individuals, develops in association with articular cartilage degeneration. Multiple factors contribute to the development of OA, including hereditary predisposition, mechanical stress, and aging[1,2]. A number of pathological changes are observed during OA development, including an imbalance between anabolic and catabolic activity of chondrocytes, increased production of cartilage-degrading enzymes such as matrix metalloproteinases (MMPs) and a disintegrin and metalloproteinase with thrombospondin motifs (ADAMTS)[3,4], and increased apoptosis[5,6] and senescence. Recent studies have suggested that chondrocyte senescence plays an important role in the pathogenesis and development of OA[7,8].

Sirtuins are nicotinamide adenine dinucleotide (NAD^+)-dependent histone and non-histone protein deacetylases with an evolutionarily conserved catalytic domain and mammalian homologs of the yeast silent information regulator 2 (Sir2)[9]. Mammals have seven sirtuins (SIRT1–SIRT7), which localize and translocate to different cellular compartments and regulate the function of a wide variety of protein substrates[10,11]. Recently, sirtuins have garnered considerable research attention owing to the variety of roles they play in aging-related diseases. Among the sirtuins, SIRT1 has been

* Address correspondence and reprint requests to: T. Matsushita, Department of Orthopaedic Surgery, Kobe University Graduate School of Medicine, 7-5-1, Kusunoki-cho, Chuo-ku, Kobe, 650-0017, Japan. Tel: 81-78-382-5985; Fax: 81-78-351-6944.

E-mail addresses: kant_kantona@yahoo.co.jp (K. Nagai), matsushi@kobe-u.ac.jp (T. Matsushita), tokiomatsuzaki@yahoo.co.jp (T. Matsuzaki), kojitakayama1978@gmail.com (K. Takayama), matsun@m4.dion.ne.jp (T. Matsumoto), kurodar@med.kobe-u.ac.jp (R. Kuroda), kurosaka@med.kobe-u.ac.jp (M. Kurosaka).

http://dx.doi.org/10.1016/j.joca.2015.03.024
1063-4584/

well studied in the context of chondrocytes and OA. Our previous studies have shown that SIRT1 inhibits apoptosis of *in vitro* human chondrocytes[12], and its inhibition in human chondrocytes leads to changes in the expression of OA-related genes[13]. Furthermore, loss of SIRT1 in chondrocytes accelerate the development of OA in mice[14]. Other studies have also shown that SIRT1 promotes cartilage-specific gene expression[15], and its overexpression in human chondrocytes inhibits changes in osteoarthritic gene expression induced by interleukin-1β[16]; these findings highlight the important roles of SIRT1 in chondrocytes and OA. On the other hand, SIRT6 has been recently implicated in DNA repair[17–19], telomere maintenance[20], attenuation of inflammation[21], and glucose homeostasis[22]. Notably, studies in mice have shown that SIRT6 deficiency produces premature aging phenotypes[17], whereas SIRT6 overexpression causes a moderate increase in the lifespan of male mice[23], strongly suggesting an important role of SIRT6 in aging and aging-associated diseases. However, its role in chondrocytes and OA has not been fully explored. The purpose of this study was to determine SIRT6 expression levels in human chondrocytes and to examine the role of SIRT6 in human chondrocytes by inhibiting SIRT6 with an RNA interference (RNAi) technique. The hypothesis was that SIRT6 exhibits protective functions toward human chondrocytes.

Materials and methods

OA and non-OA cartilage sampling and processing

OA cartilage tissues were obtained from femoral condyles of six different patients with varus knee OA during total knee arthroplasty. The cartilage samples were obtained from the distal part of both the lateral femoral condyles (LFCs) and medial femoral condyles (MFCs) of the knee joint. Lateral condyles and medial condyles were used as cartilage with mild OA and cartilage with severe OA, respectively. Articular cartilage tissues without OA were obtained from six different patients undergoing surgery for femoral neck fracture. None of the six patients had a history of joint disease, and none of the samples from these six patients showed macroscopically obvious progressed OA changes.

All OA and non-OA cartilage samples were obtained in accordance with the World Medical Association Declaration of Helsinki ethical principles for medical research involving human subjects.

Histological analysis

Cartilage tissues were fixed in 4% paraformaldehyde in 0.1 M phosphate buffered saline (PBS) for 24 h, decalcified for 2 weeks with 10% ethylenediaminetetraacetic acid (EDTA), and then embedded in paraffin wax. Each specimen was cut into 5-μm-thick slices along the sagittal plane.

For safranin-O and fast green staining, sections were stained with hematoxylin for 10 min, followed by fast green staining for 5 min and safranin-O staining for 5 min. For immunohistochemistry, deparaffinized sections were treated with 3% hydrogen peroxide to block endogenous peroxidase activity. Heat-induced epitope retrieval was performed in a citrate buffer for 20 min at 95°C. The sections were incubated with primary antibody overnight at 4°C. Following this, sections were incubated with horseradish peroxidase (HRP)-conjugated goat anti-rabbit IgG polyclonal antibody (Nichirei Bioscience, Tokyo, Japan) for 30 min at room temperature.

The signal was developed as a brown reaction product by using the peroxidase substrate 3,3′-diaminobenzidine (Nichirei Bioscience) with methyl green counterstaining, and the sections were microscopically examined. To detect SIRT6, rabbit anti-human SIRT6 antibody (Abcam) was used at a 1:100 dilution. Furthermore, to address proliferative activity of chondrocytes in human cartilage, immunostaining for proliferation cell nuclear antigen (PCNA) was performed using rabbit anti-human PCNA antibody (Abcam) at a 1:100 dilution.

Culture of human chondrocytes

Normal human knee articular chondrocytes (NHAC-kn; Lonza Walkersville, Walkersville, MD) were purchased and maintained with the Chondrocyte Growth Medium (Lonza) according to the supplier's protocol. These are human primary chondrocytes isolated from donor knee joints without any abnormalities. Each donor is assigned to one lot number and NHAC-kn of three different lot numbers was used in this study. We confirmed that these cells preserved the characteristic phenotype of normal chondrocytes, as we and others have previously reported[12,13,16,24,25]. Chondrocytes between passages three and six were used for the study.

Detection of the localization of SIRT6 in normal human chondrocytes

To detect the localization of SIRT6 in chondrocytes, immunocytochemistry was performed. Briefly, normal human chondrocytes from three donors (passage 3) were seeded onto a slide clip, and cultured for 24 h at 37°C in an incubator under 20% O_2/5% CO_2. Then, the chondrocytes were fixed with 4% paraformaldehyde in PBS for 10 min, followed by permeabilization with 0.25% Triton X-100 in PBS for another 10 min. The cells were subsequently washed with PBS, blocked with 1% bovine serum albumin (BSA) (Sigma–Aldrich) in PBS containing 0.1% Tween-20 for 1 h, and incubated with an anti-SIRT6 rabbit polyclonal (Abcam) at a 1:200 dilution for 1 h, followed by Alexa Fluor 594-conjugated goat anti-rabbit IgG (Invitrogen) at a 1:5000 dilution. After antibody staining, the cover slips were washed extensively in PBS and nuclei were counterstained with DAPI, followed by mounting as described above. Samples were viewed with a BZ-X700 (Keyence, Japan) microscope equipped with 40× objective lens and fluorescence filter sets appropriate for DAPI and Texas Red.

SIRT6 inhibition

Normal human chondrocytes from three donors ($n = 3$, passage from 3 to 6) were transfected with 100 pmol small interfering RNA (siRNA) for human SIRT6 or control non-silencing siRNA. The sense strand sequences of the RNA duplexes for human SIRT6 were as follows: No 1, 5′-CUGUCCAUCACGCUGGGUATT-3′ and No. 2, 5′-CUCACUUUGUUACUUGUUUTT-3′ (Sigma–Aldrich, Saint-Louis, Missouri, USA). Cells were seeded on a six-well plate (1.5×10^5/well) and transfected using Lipofectamine 2000 transfection reagent (Invitrogen, Carlsbad, CA, USA) according to the manufacturer's protocol. RNA or proteins were extracted 48 h after transfection.

RNA isolation and quantitative real-time PCR analysis

RNA was extracted with QIAshredder homogenizers and the RNeasy Mini kit (Qiagen, Valencia, CA, USA) according to the manufacturer's protocol, and first-strand complementary DNA (cDNA) was transcribed using High-Capacity cDNA Reverse Transcription Kit (Applied Biosystems). The converted cDNA samples (2 μL) were amplified in duplicate by quantitative real-time RT-PCR (ABI Prism 7700 Sequence Detection System) in a final volume of 25 μL using SYBR Green Master Mix reagent (Applied Biosystems).

Predesigned primers for human *SIRT6*, *MMP-1*, *MMP-2*, *MMP-3*, *MMP-9*, *MMP-13*, and *GAPDH* were obtained from Takara Bio (Shiga, Japan; Table I).

Melting curve analysis was performed using Dissociation Curves software (Applied Biosystems) to ensure that only a single product was amplified. Results were obtained using ABI Prism 7700 sequence detection software and evaluated using Excel (Microsoft, Redmond, WA, USA). The values were normalized with those for GAPDH, and relative expression was analyzed using the ΔΔCt method. The value for control siRNA expression level/GAPDH was set as 1.

RT-PCR analysis

The cDNA samples were amplified by RT-PCR in final volume of 40 μl using Ampli Taq Gold® DNA Polymerase with Gene Amp 10× PCR Buffer II and $MgCl_2$ Solution/dNTP (Applied Biosystems). The conditions for the PCR thermal cycling were as follows: 45 cycles of denaturation at 94°C for 30 s, annealing at 58°C for 30 s, and a final extension at 72°C for 60 s. The final PCR products of 20 μl were electrophoresed on a 2% agarose gel, and visualized with a LAS-3000 mini (Fujifilm, Tokyo, Japan). The primers for *COL2A1*, *COL1A1*, and *β-Actin* were obtained from Takara Bio (Shiga, Japan, Supplemental Table 1).

Protein isolation and western blotting analysis

After lipofection, normal human chondrocytes from three donors (passage 3 and 4) were lysed, and proteins were extracted with whole cell lysis buffer (Mammalian Protein Extraction Reagent, Thermo Scientific, Rockford, IL, USA) supplemented with proteinase and phosphatase inhibitor mix (Thermo Scientific) according to the manufacturer's protocol. The lysates were centrifuged at 15,000 revolutions per minute for 15 min to remove cellular debris, and the supernatants were collected.

Separated proteins were electrotransblotted onto the blotting Polyvinylidene Difluoride (PVDF) membrane (Hybond-P, GE Healthcare) with sodium dodecyl sulfate–polyacrylamide gel electrophoresis (SDS-PAGE). The membranes were probed with primary antibodies followed by an HRP-conjugated secondary antibody. Proteins were visualized with ECL Plus reagent (GE Healthcare) with a Chemilumino analyzer LAS-3000 mini (Fujifilm, Tokyo, Japan). Membranes were reprobed with anti-human α-tubulin antibody (Sigma–Aldrich) to confirm equal protein loading.

The following antibodies were used in this study: rabbit anti-human SIRT6 antibody, rabbit anti-human p21 antibody (both from Cell Signaling Technology), and mouse anti-human p16 antibody (Santa Cruz); and HRP-conjugated goat anti-rabbit IgG and HRP-conjugated goat anti-mouse IgG (both from GE Healthcare).

Table I
Primer sequences for real-time PCR analysis

Target gene	Primer sequences (5′-3′)	
	Forward	Reverse
SIRT6	CTGGTCAGCCAGAACGTGGA	CACGACTGTGTCTCGGACGTA
MMP-1	CTGGCCACCACTGCCAAATG	CTGTCCCTGAACAGCCCAGTACTTA
MMP-2	CTCATCGCAGATGCCTGGAA	CAGCCTAGCCAGTCGGATTTG
MMP-3	ATTCCATGGAGCCAGGCTTTC	CATTTGGGTCAAACTCCAACTGTG
MMP-9	ACGCACGACGTCTTCCAGTA	CCACCTGGTTCAACTCACTCC
MMP-13	TTGATGATGATGAAACCTGGACAAG	TTGCCGGTGTAGGTGTAGATAGGAA
GAPDH	GCACCGTCAAGGCTGAGAA	TGGTGAAGACGCCAGTGGA

Cell proliferation assay

The proliferation activity of normal human chondrocytes in the presence of SIRT6 siRNA and control siRNA was examined using a Cell Counting Kit-8 (CCK-8; Dojindo Laboratories, Kumamoto, Japan) according to the manufacturer's instructions. Briefly, normal human chondrocytes from three donors were seeded onto 96-well culture plates at density of 5.0×10^3 cells per well and cultured for 24 h at 37°C in an incubator under 20% O_2/5% CO_2. After the cells had been cultured for 24 h, SIRT6 and control siRNA were transfected by lipofection. CCK-8 solution was added into each well at 0, 24, 48, 72, and 96 h after lipofection respectively, and incubated for 1 h. Optical density was measured using a plate reader at 450 nm at 0, 24, 48, 72, and 96 h after lipofection ($n = 3$, passage 3, 5 and 6).

Senescence associated β-galactosidase (SA-β-Gal) assay

Cytochemical staining for SA-β-Gal was performed using a SA-β-Gal staining kit (#9860; Cell Signaling Technology). Briefly, normal human chondrocytes from three donors were seeded onto 6-well culture plates at density of 1.0×10^5 cells per well and cultured for 24 h at 37°C in an incubator under 20% O_2/5% CO_2. After the cells had been cultured for 24 h, SIRT6 and control siRNA were transfected by lipofection according to the manufacturer's instructions. Forty-eight hours after lipofection, cytochemical staining for SA-β-Gal was performed at pH 6 according to the manufacturer's protocol, and the positive cells in four randomly selected fields per treatment were counted ($n = 3$, passage 3 and 6).

Detection of γH2AX foci and telomere dysfunction-induced foci (TIFs)

To detect DNA damage and telomere dysfunction, the γH2AX foci, which represents phosphorylated histone H2AX, and TIFs where γH2AX foci co-localized with telomere repeat binding factor-1 (TRF-1) were examined 48 h after lipofection using immunofluorescence confocal microscopy, as previously described[26,27]. In brief, normal human chondrocytes from three donors (NHAC-kn, $n = 3$, passage 3) were seeded onto cover slips and cultured for 24 h at 37°C in an incubator under 20% O_2/5% CO_2. After the cells had been cultured for 24 h, SIRT6 or control siRNA were transfected by lipofection according to the manufacturer's instructions. Forty-eight hours after lipofection, chondrocytes were fixed for 10 min with 4% paraformaldehyde in PBS, followed by permeabilization with 0.25% Triton X-100 in PBS for 10 min. The cells were subsequently washed with PBS, blocked for 1 h with 1% BSA (Sigma–Aldrich) in PBS containing 0.1% Tween-20, and then incubated for 1 h with an anti-TRF-1 mouse monoclonal antibody (clone TRF-78, Abcam) at a 1:1000 dilution, followed by a goat anti-mouse IgG-Alexa Fluor 488 conjugate (Invitrogen) at a 1:1000 dilution. Before incubation with the second primary antibody, the cells were thoroughly washed in PBS/0.1% Tween-20, post-fixed with 4% paraformaldehyde for 15 min, washed again with PBS, and then incubated for a further 15 min with 25 mM glycine in PBS to inactivate the paraformaldehyde.

γH2AX was detected by incubation with a rabbit polyclonal antibody raised against a synthetic phosphopeptide mapping to residues surrounding Ser139 of human histone H2A.X (Cell Signaling) at a 1:100 dilution, followed by Alexa Fluor 594-conjugated goat anti-rabbit IgG (Invitrogen) at a 1:5000 dilution. After antibody staining, the cover slips were washed extensively in PBS/0.1% Tween-20 and nuclei were counterstained with DAPI, followed by mounting as described above.

Samples were viewed with a LSM700 (Zeiss, Germany) microscope equipped with 40× objective lens and fluorescence filter sets as appropriate for viewing DAPI, fluorescein, and Texas Red staining

(UV-2E/C, B-2E/C, and G-2E/C, respectively). Z-stack fluorescence images were captured using the Zen software. Digital microphotographs of 20 fields randomly selected from both chondrocytes transfected with control siRNA and SIRT6 siRNA were obtained, and images of each chondrocyte were captured. The average area of γH2AX foci per cell for each treatment was automatically calculated using ImageJ software (http://rsbweb.nih.gov/ij/). In addition, the number of TIFs per cell was counted manually and then averaged. Twenty nuclei from the chondrocytes transfected with SIRT6 siRNA and control siRNA were examined in each donor.

Statistical analysis

All data were expressed as the mean ± 95% confidence interval (95% CI). The results were analyzed using StatView 5.0 (Abacus Concepts Inc., Berkeley, CA, USA). Comparisons between two groups were made using *t*-test. The normality and homogeneity of variance of data were tested before statistical analysis. When the conditions for data properties were fulfilled, *t*-test was used. A P value <0.05 was considered statistically significant.

Results

SIRT6-positive chondrocytes were observed in human cartilage samples and cultured human chondrocytes

Immunohistochemical analysis showed that SIRT6-positive cells were present in normal cartilage, and in mild and severe OA cartilage obtained from elderly patients [Fig. 1(A) and (B)]. SIRT6 expression was localized to the nucleus and mainly expressed in the superficial zone of articular cartilage. Representative results were obtained from six different patients for FH and six different OA patients for MFC and LFC. Immunofluorescence analysis also showed that SIRT6 was expressed in human chondrocytes and localized to the nucleus [Fig. 1(C)].

Depletion of SIRT6 induced up-regulation of MMP-1 and MMP-13

The *SIRT6* mRNA level was significantly reduced to approximately 40% by SIRT6 siRNA transfection (1 vs 0.41 ± 0.04, $n = 3$, $P = 0.001$). The SIRT6 protein level was also markedly reduced by SIRT6 siRNA, showing that SIRT6 was efficiently inhibited by SIRT6 siRNA [Fig. 2(A)]. In the real-time PCR analysis, the depletion of SIRT6 significantly increased *MMP-1* (1 vs 2.3 ± 0.5, $P = 0.03$) and *MMP-13* mRNA expression (1 vs 4.7 ± 0.4, $P = 0.01$), but no significant changes were observed in *MMP-2* (1 vs 1.0 ± 0.1, $P = 0.74$), *MMP-3* (1 vs 1.1 ± 0.1, $P = 0.15$), or *MMP-9* expression (1 vs 1.2 ± 0.3, $P = 0.30$) [Fig. 2(C)]. Similar results were obtained with a different sequence of siRNA for *SIRT6* (Supplemental Fig. 1(A), (B)).

Depletion of SIRT6 caused premature senescence and the decrease of proliferation activity

Immunohistochemical analysis showed that SIRT6 was strongly expressed in chondrocytes, forming clusters that also expressed

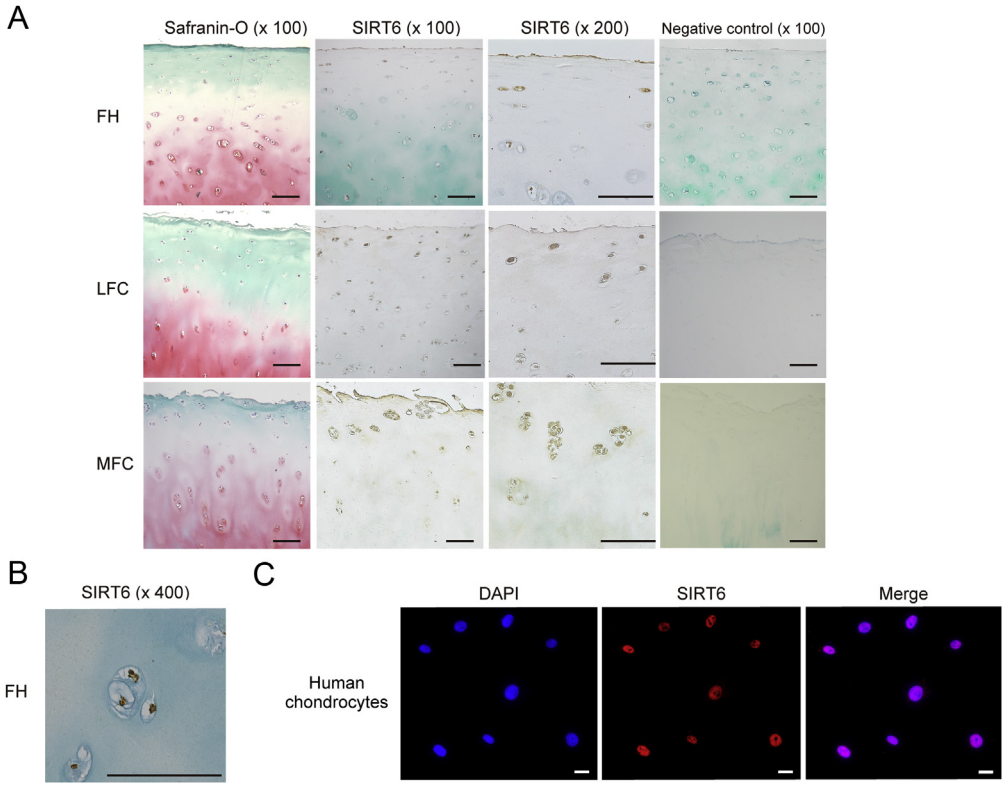

Fig. 1. SIRT6 expression in articular cartilages and cultured chondrocytes (A) Microscopic images of Safranin-O, Immunohistochemistry for SIRT6 and negative control (scale bars = 100 μm). Cartilage samples are MFC and LFC from a 72-year-old female patient with varus OA, and femoral head (FH) from a 74-year-old female patient with femoral neck fracture. The chondrocytes with brown-colored nucleus were positive. Representative results were obtained from six different patients for FH and six different OA patients for MFC and LFC. (B) A microscopic image of immunohistochemistry of the FH for SIRT6 taken at a high magnification (×400). SIRT6 was localized to the nucleus (Scale bar = 100 μm). (C) Microscopic images of cultured human chondrocytes immunostained with antibodies against SIRT6 (red) counterstained with DAPI (blue), and merged images of DAPI and SIRT6 (scale bars = 20 μm). Immunofluorescence analysis showed that SIRT6 was expressed in human chondrocytes and localized to the nucleus. Representative results were obtained from repeated experiment using human chondrocytes from three different donors.

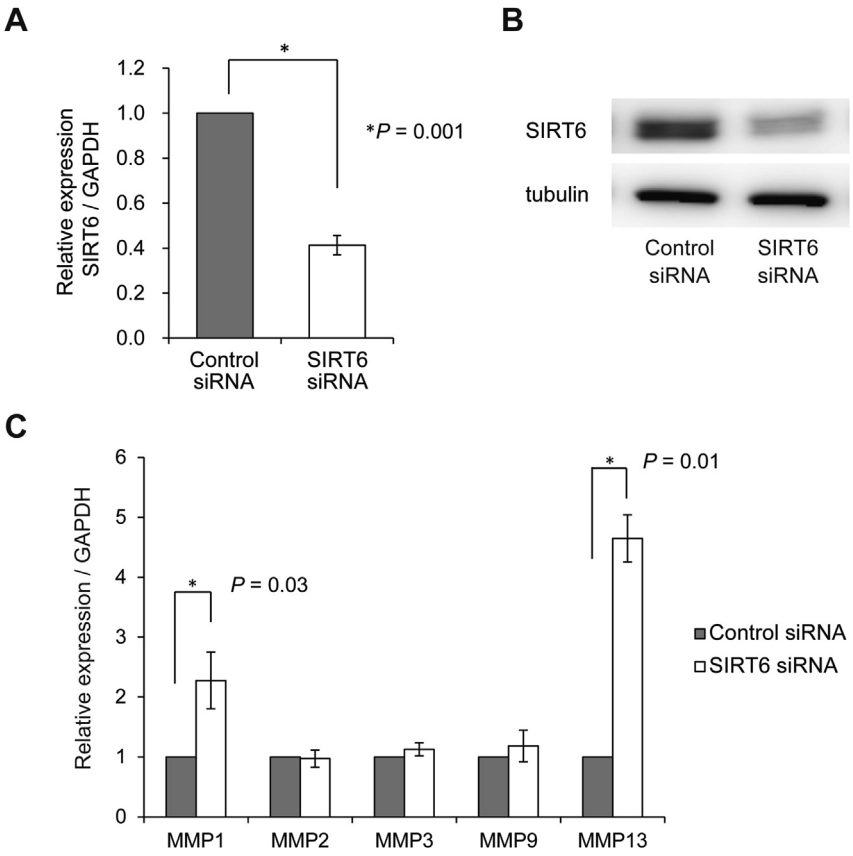

Fig. 2. The efficiency and influence of SIRT6 inhibition by SIRT6 siRNA (A) Real-time PCR analysis for *SIRT6* mRNA in normal human chondrocytes. The *SIRT6* mRNA level was significantly reduced to approximately 40% by SIRT6 siRNA transfection. Non-silencing siRNA was used as a control. *Statistically significant difference ($n = 3$, $P = 0.001$). GAPDH was used as endogenous control. The value for control expression level/GAPDH was set as 1. Values are the mean ± 95% CI. (B) Western blotting analysis for SIRT6 in normal human chondrocytes. Tubulin was served as a control. Representative results are shown from three different donors. (C) Real-time PCR analysis for the expression of MMP family members. *MMP-1* and *13* mRNA were significantly increased by the SIRT6 depletion. GAPDH was used as endogenous control. The value for control siRNA expression level/GAPDH was set as 1. Values are the mean ± 95% CI. *Statistically significant difference ($n = 3$, $P = 0.03$ and $P = 0.01$ respectively).

PCNA in severely damaged OA cartilage [Fig. 3(A)]. This finding suggests a role of SIRT6 in chondrocyte proliferation, which we proceeded to investigate.

The proliferation assay showed that the absorbance of the siRNA group was significantly lower than that of controls at 72 and 96 h after lipofection (0.77 ± 0.06 vs 0.99 ± 0.06, $P = 0.02$ and 1.16 ± 0.11 vs1.53 ± 0.10, $P = 0.002$, respectively. $n = 3$), [Fig. 3(B)], indicating that proliferation was reduced when SIRT6 was depleted. Furthermore, the SA-β-Gal assay showed that the percentage of SA-β-Gal-positive cells was significantly higher in the SIRT6 siRNA group (24.3 ± 4.2%) than in the control group (11.3 ± 3.0%) ($n = 3$, $P = 0.008$; Fig. 3(C)), indicating that the depletion of SIRT6 induced premature senescence.

Depletion of SIRT6 caused accumulation of γH2AX foci and TIFs

To elucidate the mechanism by which depletion of SIRT6 reduces proliferation and induces premature senescence, we examined whether depletion of SIRT6 results in the accumulation of γH2AX foci and TIFs, which form at sites of DNA damage and dysfunctional telomeres. Immunofluorescence microscopic analyses showed that γH2AX foci and TIFs were increased in the SIRT6-depleted chondrocytes than in controls [Fig. 4(A)]. The relative area of γH2AX was significantly greater in the SIRT6-depleted chondrocytes (1.9 ± 0.1/cell) than in control chondrocytes (1.0 ± 0.1/cell) ($n = 3$, $P = 0.0001$; Fig. 4(B)). In addition, the average number of TIFs per cell was significantly higher in the SIRT6-depleted chondrocytes (3.5 ± 0.8/cell) than in control chondrocytes (1.3 ± 0.2/cell) ($n = 3$, $P = 0.007$; Fig. 4(C)).

Depletion of SIRT6 up-regulated p16, but not p21

To examine the downstream signaling pathways that mediate the induction of senescence by SIRT6 depletion, we used western blotting to assess the protein levels of mediators for DNA damage-induced senescence, cyclin-dependent kinase inhibitors (CDKIs) p16 and p21. The p16 protein level was higher and p21 protein level was lower in the SIRT6-depleted chondrocytes than those in control chondrocytes (Fig. 5). Results are representative of experiments performed using three different donors.

Discussion

To the best of our knowledge, this is the first study to show a role of SIRT6 in human chondrocytes. In the first step of the study, SIRT6 expression in human chondrocytes was confirmed by immunohistochemistry. SIRT6 was localized to the nucleus in human chondrocytes, similar to that previously reported by Michishita *et al.* who showed the localization of SIRT6 to the nucleus in normal human fibroblast[28]. Additionally, SIRT6 was mainly expressed in the superficial zone of cartilage, where chondrocytes are directly under stress. SIRT6 was also strongly expressed in the PCNA-positive chondrocytes that form clusters in OA cartilage. Formation of clusters is a characteristic feature observed during

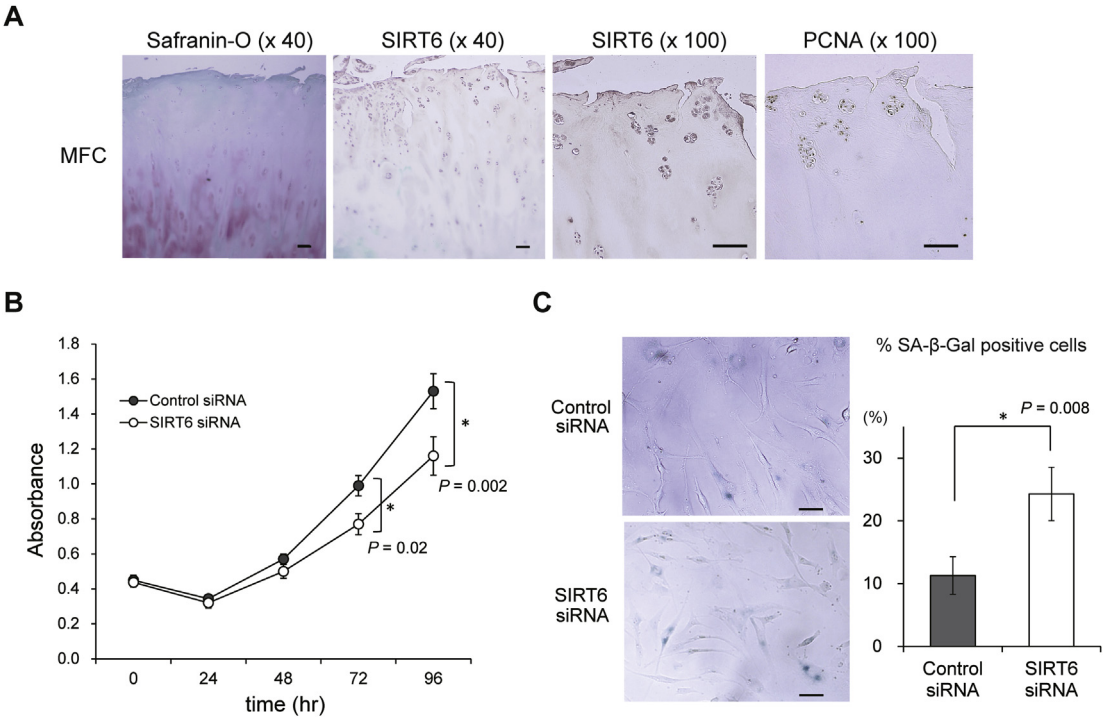

Fig. 3. The influence of the depletion of SIRT6 on proliferation and senescence. (A) The expression of SIRT6 and PCNA in articular cartilage of MFC from a 72-year-old female patient with varus OA. Safranin-O, Immunohistochemistry for SIRT6 at ×40 and ×100, and for PCNA at ×100. SIRT6 was strongly expressed in chondrocytes forming clusters that also express PCNA. (Scale bars = 100 μm). Representative results are shown from six repeated experiments from six different patients. (B) Proliferation activity assay using Cell Counting Kit-8. Depletion of SIRT6 significantly reduced proliferation activity 72 and 96 h after lipofection. Values are the mean ± 95% CI of the data obtained from three donors. *Statistically significant difference ($n = 3$, $P = 0.02$ and $P = 0.002$ respectively). (C) SA-β-Gal assay. The percentage of SA-β-Gal positive cells was significantly higher in the SIRT6 siRNA group compared with the control group. Values are the mean ± 95% CI of the data obtained from three donors. (Scale bar = 100 μm). *Statistically significant difference ($n = 3$, $P = 0.008$).

progression of OA, and the chondrocytes in these clusters are proliferating clonal chondrocytes[29]. It has been suggested this is a self-reparatory process[30], which implies that SIRT6 plays a role in the proliferation of chondrocytes.

As a second step, we examined the effects of inhibiting SIRT6 in human chondrocytes *in vitro* to elucidate the role of SIRT6. Inhibition of SIRT6 reduced proliferation of human chondrocytes. Recently, Piao *et al.* reported that the thickness of the proliferating zone and the hypertrophic zone of the growth plate is reduced in *Sirt6*-deficient mice[31] and that inhibition of Sirt6 reduces expression of cyclin D1 and D2, and Indian hedgehog signaling in mouse epiphyseal chondrocytes. These reports support the idea that SIRT6 is an important regulator for chondrocyte proliferation.

Inhibition of SIRT6 also increased senescence of chondrocytes. Similar protective roles of SIRT6 have been reported in other types of cells such as endothelial cells[27], induced pluripotent stem cells[32], and fibroblasts[33], although the descriptions of the underlying mechanisms of the regulation of senescence by SIRT6 differ. We observed that depletion of SIRT6 led to accumulation of DNA damage and telomere dysfunction, as detected by increased γH2AX-positive areas and TIFs. These observations suggest that increased DNA damage and telomere dysfunction resulted in subsequent DNA damage responses and eventual cellular senescence. In support of this idea, several studies have described the mechanisms through which SIRT6 promotes DNA repair and protects from telomere dysfunction. SIRT6 contributes to DNA double-strand break repair by controlling mobilization of a DNA double-strand break repair factor[18] or by interacting with poly[ADP–ribose] polymerase 1[19] in response to DNA damage. In addition, SIRT6 prevents telomere dysfunction through deacetylation at telomeres[20]. These findings, together with our observations, suggest that SIRT6 prevents premature senescence of human chondrocytes by controlling DNA repair and maintaining proper telomere function.

Two cell-cycle inhibitors that are often expressed by senescent cells are the CDKIs p21 and p16[34–36]. These CDKIs are components of tumor-suppressor pathways that are governed by the p53 and retinoblastoma (pRB) proteins, respectively. Both the p21 pathway and the p16 pathway can establish and maintain growth arrest, which is a typical feature of cellular senescence[37]. DNA damage is one of the many stimuli that induce senescence, and DNA-damage initiated senescence depends on p53 and is usually accompanied by the expression of p21[26,38]. However, in many types of cells, DNA damage and telomere dysfunction also induce p16, which provides a second barrier to block cell growth with severely damaged DNA or dysfunctional telomeres[39–41]. This is an essential role in prevention of senescence.

The relationship between p16 and OA was revealed in a study by Zhou *et al.*[42] who reported that p16-positive cells are more plentiful in OA chondrocytes than in age-matched normal tissue. In addition, siRNA knockdown of p16 in OA chondrocytes decreases senescent features while promoting proliferation of chondrocytes and matrix gene expression[42]. This finding indicates that p16 is involved in the pathogenesis of OA. In the present study, the p16 protein level was increased by the SIRT6 depletion, but the p21 protein level was not, which suggests that SIRT6 protects human chondrocytes from senescence via the p16-pRB pathway. It is intriguing that the level of p16 was increased whereas that of another senescence regulator, p21, was decreased in the senescent cells. Stein *et al.*[41] showed a differential role of CDK inhibitors p21 and p16 in the regulation of senescence and differentiation in human fibroblasts. They observed that p21 was up-regulated during the early stage of senescence,

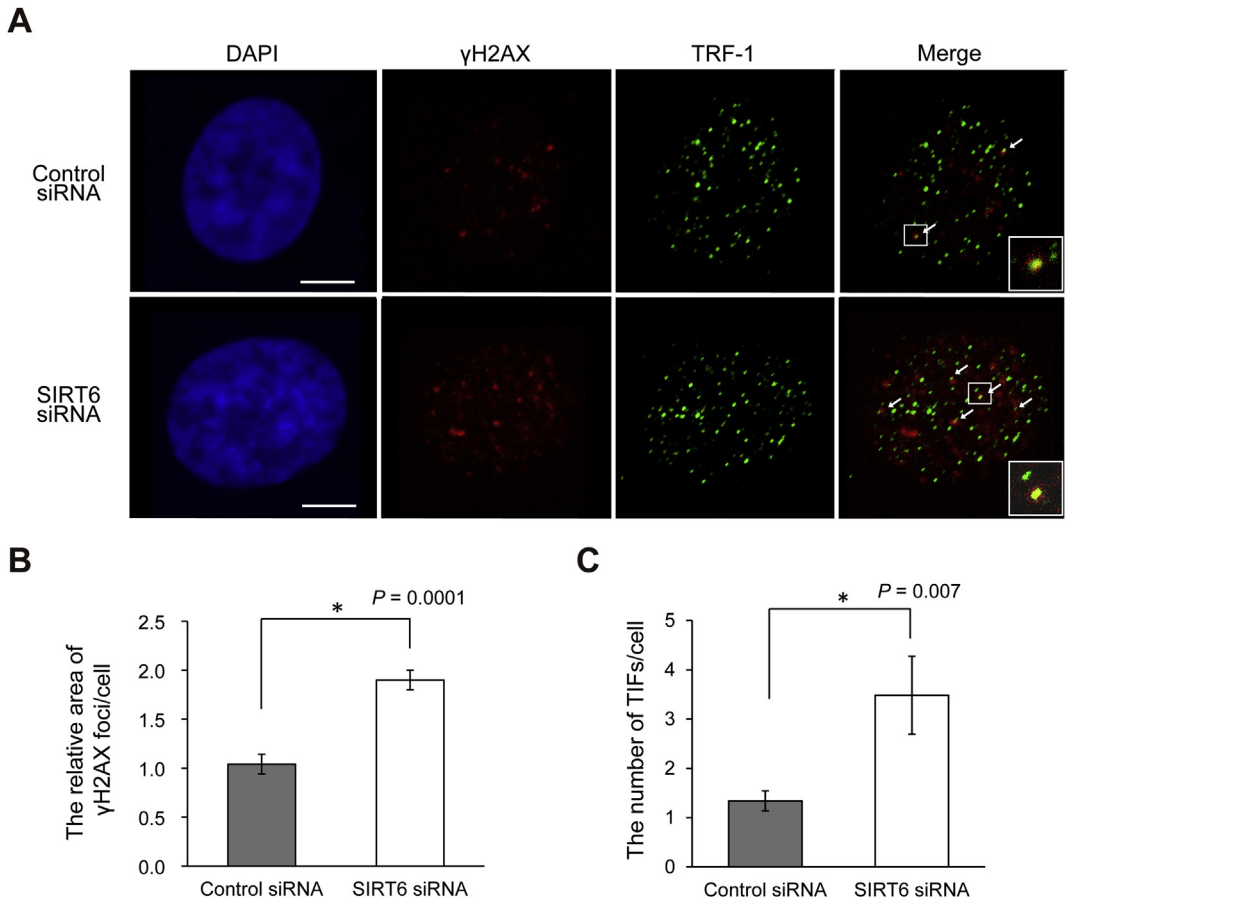

Fig. 4. The influence of the depletion of SIRT6 on DNA damage and telomere dysfunction. (A) Microscopic images of control siRNA and SIRT6 siRNA chondrocytes immunostained with antibodies against γH2AX (red) and TRF-1 (green), and counterstained with DAPI (blue). White arrows in the merged images point to sites of co-localization which means TIFs. Scale bars = 5 μm γH2AX foci and TIFs were increased in the SIRT6-depleted chondrocytes than in controls. Representative results are shown from four repeated experiments using chondrocytes from three different donors. (B) Quantification of γH2AX foci expressed as mean relative area per cell. Twenty nuclei from the chondrocytes transfected with SIRT6 siRNA and control siRNA were examined. The relative area of γH2AX foci was significantly greater in the SIRT6-depleted chondrocytes than in control chondrocytes. Values are the mean ± 95% CI. *Statistically significant difference ($n = 3$, $P = 0.0001$). (C) Quantification of TIFs per cell. Twenty nuclei from the chondrocytes transfected with SIRT6 siRNA and control siRNA were examined in each donor. The average number of TIFs per cell was significantly higher in the SIRT6-depleted chondrocytes than in control chondrocytes. Values are the mean ± 95% CI. *Statistically significant difference ($n = 3$, $P = 0.007$).

whereas once senescence was achieved, p21 decreased and p16 increased. Thus, they concluded that the up-regulation of p16 might be essential for maintenance of the senescent cell-cycle arrest. Thus, we speculate that senescence might have been already achieved at the time of the extraction of protein, causing the discrepancy between the levels of p16 and p21 in SIRT6-deficient chondrocytes in the present study.

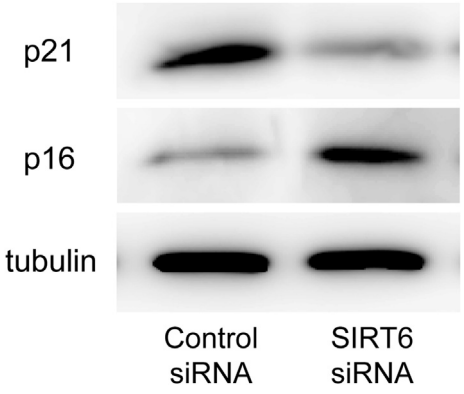

Fig. 5. Western blotting for p16 and p21. The p16 protein level was higher and the p21 protein level was lower in the SIRT6-depleted chondrocytes than in control chondrocytes. Representative results were obtained from three different donors. Tubulin was used as a control.

We also observed increased expression of *MMP-1* and *MMP-13* mRNA associated with inhibition of SIRT6. MMP-1 and MMP-13 are classic collagenases. In particular, MMP-13 is a major mediator of type 2 collagen cleavage, and significant roles for MMP-13 in the development of OA have been suggested[43–46]. In addition, it has been reported that immunostaining for MMP-1 and MMP-13 in cartilage is increased in association with aging[47]. The regulatory mechanism underlying MMP-1 and MMP-13 expression is intriguing. SIRT6 is known to regulate the nuclear factor kappaB (NF-kB) pathway, a major mediator for inflammatory responses. Therefore, it is possible that *MMP-1* and *MMP-13* expression were increased through the regulation of NF-kB[21]. Furthermore, cells undergoing a senescent process often exhibit characteristic phenotypic changes such as increased MMPs and interleukins[8], referred to as the senescent secretory phenotype[36,37]. Therefore, it is also possible that the increased *MMP-1* and *MMP-13* expression is associated with phenotypic changes of the SIRT6-depleted chondrocytes to the senescent secretory phenotype. Further studies are required to elucidate the mechanism of the regulation of MMP-1 and MMP-13 by SIRT6.

It should be noted that current our study has a limitation. Although human chondrocytes extracted from healthy donors were used for the experiments *in vitro*, the chondrocytes were partially de-differentiated and fibroblastic as RT-PCR analysis showed a decreased COL2A1/COL1A1 ratio (Supplemental Fig. 2). Therefore, our results may be limited to chondrocytes that show some level of de-differentiation. However, considering one of the characteristic observations during progression of OA that chondrocytes become fibroblastic, we believe that our study provides insight into the role of SIRT6 in the regulation of human chondrocyte senescence and pathogenesis of OA despite this limitation.

In conclusion, we demonstrated that depletion of SIRT6 in human chondrocytes decreased proliferation while inducing premature senescence. In addition, depletion of SIRT6 led to accumulation of DNA damage and telomere dysfunction. Our observations suggest that SIRT6 plays an important role in protecting chondrocytes from premature senescence, DNA damage, and telomere dysfunction. Further studies of the role of SIRT6 in senescence of human chondrocytes may help elucidate the pathogenesis of OA, and confirm the potential of SIRT6 as a new therapeutic target for OA.

Authors' contributions

All authors have made substantial contributions to (1) the conception and design of the study, or acquisition of data, or analysis and interpretation of data; (2) drafting the article or revising it critically for important intellectual content; and (3) final approval of the version to be submitted. The specific contributions of the authors are as follows:

(1) Conception and design of the study: KN, TMatsushita, TMatsuzaki, KT, TMatsumoto, RK, MK
(2) Analysis and interpretation of the data: KN, TMatsushita, TMatsuzaki, KT, TMatsumoto, RK, MK
(3) Drafting of the article: KN, TMatsushita, TMatsuzaki, KT
(4) Critical revision of the article for important intellectual content: KN, TMatsushita, TMatsuzaki, KT, TMatsumoto, RK, MK
(5) Final approval of the article: KN, TMatsushita, TMatsuzaki, KT, TMatsumoto, RK, MK
(6) Statistical expertise: KN, TMatsushita, TMatsuzaki
(7) Collection and assembly of data: KN, TMatsuzaki

Funding
There was no funding source in this study.

Competing interest
The authors declare that we have no competing interests.

Acknowledgments

We would like to thank Ms. Kyoko Tanaka, Ms. Maya Yasuda and Ms. Minako Nagata for their expert technical assistance.

Supplementary data

Supplementary data related to this article can be found at http://dx.doi.org/10.1016/j.joca.2015.03.024.

References

1. Goldring MB, Goldring SR. Osteoarthritis. J Cell Physiol 2007;213:626–34.
2. Aigner T, Sachse A, Gebhard PM, Roach HI. Osteoarthritis: pathobiology-targets and ways for therapeutic intervention. Adv Drug Deliv Rev 2006;58:128–49.
3. Cawston TE, Wilson AJ. Understanding the role of tissue degrading enzymes and their inhibitors in development and disease. Best Pract Res Clin Rheumatol 2006;20:983–1002.
4. Plaas A, Osborn B, Yoshihara Y, Bai Y, Bloom T, Nelson F, *et al.* Aggrecanolysis in human osteoarthritis: confocal localization and biochemical characterization of ADAMTS5-hyaluronan complexes in articular cartilages. Osteoarthritis Cartilage 2007;15:719–34.
5. Blanco FJ, Guitian R, Vazquez-Martul E, de Toro FJ, Galdo F. Osteoarthritis chondrocytes die by apoptosis. A possible pathway for osteoarthritis pathology. Arthritis Rheum 1998;41:284–9.
6. Kim HA, Lee YJ, Seong SC, Choe KW, Song YW. Apoptotic chondrocyte death in human osteoarthritis. J Rheumatol 2000;27:455–62.
7. Dai SM, Shan ZZ, Nakamura H, Masuko-Hongo K, Kato T, Nishioka K, *et al.* Catabolic stress induces features of chondrocyte senescence through overexpression of caveolin 1: possible involvement of caveolin 1-induced down-regulation of articular chondrocytes in the pathogenesis of osteoarthritis. Arthritis Rheum 2006;54:818–31.
8. Loeser RF. Aging and osteoarthritis: the role of chondrocyte senescence and aging changes in the cartilage matrix. Osteoarthritis Cartilage 2009;17:971–9.
9. Imai S, Armstrong CM, Kaeberlein M, Guarente L. Transcriptional silencing and longevity protein Sir2 is an NAD-dependent histone deacetylase. Nature 2000;403:795–800.
10. Haigis MC, Guarente LP. Mammalian sirtuins–emerging roles in physiology, aging, and calorie restriction. Genes Dev 2006;20:2913–21.
11. Nakagawa T, Guarente L. Sirtuins at a glance. J Cell Sci 2011;124:833–8.
12. Takayama K, Ishida K, Matsushita T, Fujita N, Hayashi S, Sasaki K, *et al.* SIRT1 regulation of apoptosis of human chondrocytes. Arthritis Rheum 2009;60:2731–40.
13. Fujita N, Matsushita T, Ishida K, Kubo S, Matsumoto T, Takayama K, *et al.* Potential involvement of SIRT1 in the pathogenesis of osteoarthritis through the modulation of chondrocyte gene expressions. J Orthop Res 2011;29:511–5.
14. Matsuzaki T, Matsushita T, Takayama K, Matsumoto T, Nishida K, Kuroda R, *et al.* Disruption of Sirt1 in chondrocytes causes accelerated progression of osteoarthritis under mechanical stress and during ageing in mice. Ann Rheum Dis 2013, http://dx.doi.org/10.1136/annrheumdis-2012-202620.
15. Dvir-Ginzberg M, Gagarina V, Lee EJ, Hall DJ. Regulation of cartilage-specific gene expression in human chondrocytes by SirT1 and nicotinamide phosphoribosyltransferase. J Biol Chem 2008;283:36300–10.
16. Matsushita T, Sasaki H, Takayama K, Ishida K, Matsumoto T, Kubo S, *et al.* The overexpression of SIRT1 inhibited osteoarthritic gene expression changes induced by interleukin-1beta in human chondrocytes. J Orthop Res 2013;31:531–7.
17. Mostoslavsky R, Chua KF, Lombard DB, Pang WW, Fischer MR, Gellon L, *et al.* Genomic instability and aging-like phenotype in the absence of mammalian SIRT6. Cell 2006;124:315–29.
18. McCord RA, Michishita E, Hong T, Berber E, Boxer LD, Kusumoto R, *et al.* SIRT6 stabilizes DNA-dependent protein kinase at chromatin for DNA double-strand break repair. Aging 2009;1:109–21.
19. Mao Z, Hine C, Tian X, Van Meter M, Au M, Vaidya A, *et al.* SIRT6 promotes DNA repair under stress by activating PARP1. Science 2011;332:1443–6.

20. Michishita E, McCord RA, Berber E, Kioi M, Padilla-Nash H, Damian M, *et al*. SIRT6 is a histone H3 lysine 9 deacetylase that modulates telomeric chromatin. Nature 2008;452:492–6.
21. Kawahara TL, Michishita E, Adler AS, Damian M, Berber E, Lin M, *et al*. SIRT6 links histone H3 lysine 9 deacetylation to NF-kappaB-dependent gene expression and organismal life span. Cell 2009;136:62–74.
22. Zhong L, D'Urso A, Toiber D, Sebastian C, Henry RE, Vadysirisack DD, *et al*. The histone deacetylase Sirt6 regulates glucose homeostasis via Hif1alpha. Cell 2010;140:280–93.
23. Kanfi Y, Naiman S, Amir G, Peshti V, Zinman G, Nahum L, *et al*. The sirtuin SIRT6 regulates lifespan in male mice. Nature 2012;483:218–21.
24. Hashimoto S, Nishiyama T, Hayashi S, Fujishiro T, Takebe K, Kanzaki N, *et al*. Role of p53 in human chondrocyte apoptosis in response to shear strain. Arthritis Rheum 2009;60:2340–9.
25. Sasaki H, Takayama K, Matsushita T, Ishida K, Kubo S, Matsumoto T, *et al*. Autophagy modulates osteoarthritis-related gene expression in human chondrocytes. Arthritis Rheum 2012;64:1920–8.
26. Herbig U, Jobling WA, Chen BP, Chen DJ, Sedivy JM. Telomere shortening triggers senescence of human cells through a pathway involving ATM, p53, and p21(CIP1), but not p16(INK4a). Mol Cell 2004;14:501–13.
27. Cardus A, Uryga AK, Walters G, Erusalimsky JD. SIRT6 protects human endothelial cells from DNA damage, telomere dysfunction, and senescence. Cardiovasc Res 2013;97:571–9.
28. Michishita E, Park JY, Burneskis JM, Barrett JC, Horikawa I. Evolutionarily conserved and nonconserved cellular localizations and functions of human SIRT proteins. Mol Biol Cell 2005;16:4623–35.
29. Kouri JB, Jimenez SA, Quintero M, Chico A. Ultrastructural study of chondrocytes from fibrillated and non-fibrillated human osteoarthritic cartilage. Osteoarthritis Cartilage 1996;4:111–25.
30. Lotz MK, Otsuki S, Grogan SP, Sah R, Terkeltaub R, D'Lima D. Cartilage cell clusters. Arthritis Rheum 2010;62:2206–18.
31. Piao J, Tsuji K, Ochi H, Iwata M, Koga D, Okawa A, *et al*. Sirt6 regulates postnatal growth plate differentiation and proliferation via Ihh signaling. Sci Rep 2013;3:3022.
32. Sharma A, Diecke S, Zhang WY, Lan F, He C, Mordwinkin NM, *et al*. The role of SIRT6 protein in aging and reprogramming of human induced pluripotent stem cells. J Biol Chem 2013;288:18439–47.
33. Mao Z, Tian X, Meter M, Ke Z, Gorbunova V, Seluanov A. Sirtuin 6 (SIRT6) rescues the decline of homologous recombination repair during replicative senescence. Proc Natl Acad Sci USA 2012;109:11800–5.
34. Campisi J. Cellular senescence as a tumor-suppressor mechanism. Trends Cell Biol 2001;11:S27–31.
35. Muller M. Cellular senescence: molecular mechanisms, in vivo significance, and redox considerations. Antioxid Redox Signal 2009;11:59–98.
36. Campisi J. Senescent cells, tumor suppression, and organismal aging: good citizens, bad neighbors. Cell 2005;120:513–22.
37. Campisi J, d'Adda di Fagagna F. Cellular senescence: when bad things happen to good cells. Nat Rev Mol Cell Biol 2007;8:729–40.
38. Di Leonardo A, Linke SP, Clarkin K, Wahl GM. DNA damage triggers a prolonged p53-dependent G1 arrest and long-term induction of Cip1 in normal human fibroblasts. Genes Dev 1994;8:2540–51.
39. Beausejour CM, Krtolica A, Galimi F, Narita M, Lowe SW, Yaswen P, *et al*. Reversal of human cellular senescence: roles of the p53 and p16 pathways. EMBO J 2003;22:4212–22.
40. Jacobs JJ, de Lange T. Significant role for p16INK4a in p53-independent telomere-directed senescence. Curr Biol 2004;14:2302–8.
41. Stein GH, Drullinger LF, Soulard A, Dulic V. Differential roles for cyclin-dependent kinase inhibitors p21 and p16 in the mechanisms of senescence and differentiation in human fibroblasts. Mol Cell Biol 1999;19:2109–17.
42. Zhou HW, Lou SQ, Zhang K. Recovery of function in osteoarthritic chondrocytes induced by p16INK4a-specific siRNA in vitro. Rheumatology (Oxford) 2004;43:555–68.
43. Mitchell PG, Magna HA, Reeves LM, Lopresti-Morrow LL, Yocum SA, Rosner PJ, *et al*. Cloning, expression, and type II collagenolytic activity of matrix metalloproteinase-13 from human osteoarthritic cartilage. J Clin Invest 1996;97:761–8.
44. Billinghurst RC, Dahlberg L, Ionescu M, Reiner A, Bourne R, Rorabeck C, *et al*. Enhanced cleavage of type II collagen by collagenases in osteoarthritic articular cartilage. J Clin Invest 1997;99:1534–45.
45. Little CB, Barai A, Burkhardt D, Smith SM, Fosang AJ, Werb Z, *et al*. Matrix metalloproteinase 13-deficient mice are resistant to osteoarthritic cartilage erosion but not chondrocyte hypertrophy or osteophyte development. Arthritis Rheum 2009;60:3723–33.
46. Kevorkian L, Young DA, Darrah C, Donell ST, Shepstone L, Porter S, *et al*. Expression profiling of metalloproteinases and their inhibitors in cartilage. Arthritis Rheum 2004;50:131–41.
47. Wu W, Billinghurst RC, Pidoux I, Antoniou J, Zukor D, Tanzer M, *et al*. Sites of collagenase cleavage and denaturation of type II collagen in aging and osteoarthritic articular cartilage and their relationship to the distribution of matrix metalloproteinase 1 and matrix metalloproteinase 13. Arthritis Rheum 2002;46:2087–94.